Characteristics of magnetorheological fluids under single and mixed modes

El-Wahed, Ali; Balkhoyor, Loaie

Published in:
Proceedings of the Institution of Mechanical Engineering, Part C: Journal of Mechanical Engineering Science

DOI:
10.1177/0954406216653621

Publication date:
2017

Document Version
Peer reviewed version

Characteristics of magnetorheological fluids under single and mixed modes

Dr. Ali El Wahed[1] and Loaie Balkhoyor[2]

[1]Corresponding Author

Mechanical Engineering, School of Science & Engineering, University of Dundee, Dundee DD1 4HN, U.K.

Tel. +44 (0) 1382 384496; fax +44 (0) 1382 384389

E-mail address: a.elwahed@dundee.ac.uk

[2]PhD student in the Mechanical Engineering & Mechatronics Department, University of Dundee, Dundee DD1 4HN, U.K.

Tel. +44 (0) 1382 384496; fax +44 (0) 1382 384389

E-mail address: l.balkhoyor@dundee.ac.uk

ABSTRACT

Rheological properties of magnetorheological (MR) fluids can be changed by application of external magnetic fields. These dramatic and reversible field-induced rheological changes permit the construction of many novel electromechanical devices having potential utility in the automotive, aerospace, medical, and other fields. Vibration control is regarded as one of the most successful engineering applications of MR devices, most of which have exploited the variable shear, flow, or squeeze characteristics of MR fluids. These fluids may have even greater potential for applications in vibration control if utilized under a mixed-mode operation. This paper presents results of an experimental investigation conducted using MR fluids operated under dynamic squeeze, shear-flow, and mixed modes. A special MR fluid cell comprising a cylinder, which served as a reservoir for the fluid, and a piston was designed

and tested under constant input displacement using a high-strength tensile machine for various magnetic field intensities. Under vertical piston motions, the MR fluid sandwiched between the parallel circular planes of the cell was subjected to compressive and tensile stresses, whereas the fluid contained within the annular gap was subjected to shear flow stresses. The magnetic field required to energize the fluid was provided by a pair of toroidally shaped coils, located symmetrically about the centerline of the piston and cylinder. This arrangement allows individual and simultaneous control of the fluid contained in the circular and cylindrical fluid gaps; consequently, the squeeze mode, shear-flow mode, or mixed-mode operation of the fluid could be activated separately. The performance of these fluids was found to depend on the strain direction. Additionally, the level of transmitted force was found to improve significantly under mixed-mode operation of the fluid.

Keywords: A. Magnetorheological fluids, C. Mixed mode, G. Strain direction

Introduction

Magnetorheological (MR) and electrorheological (ER) fluids belong to a class of smart fluids whose rheological properties can be reversibly controlled through the application and removal of magnetic and electric fields, respectively [1,2]. Both these kinds of fluids contain solid particles, typically micrometer sized, suspended in a carrier liquid. Application of an external field across these fluids causes the particles to arrange themselves into chains that are parallel to the direction of the field, which enhances the apparent viscosity and yield stress of these fluids. The ability of these field-controllable fluids, utilized in controllable electromechanical devices, to alter their properties in a fraction of a millisecond gives them an important advantage over other mechanical devices. As a result, they have been employed in an on-going research over the past two to three decades with the aim of investigating their engineering applications. Vibration control is considered to be the most promising application for the large-scale commercial exploitation of these fluids [3]. For example, progress has been made in developing long-stroke MR and ER vibration suppression devices [4,5]. The majority of these fluids have been utilized in either the simple flow mode [6,7] or the shear [8,9] mode of operation. An alternative arrangement—the squeeze mode—in which the fluid is subjected to compressive and tensile stresses in a direction parallel to the applied field, has been proposed for short-stroke damping applications [10,11]. It has been shown that the yield stress in this mode is greater by an order of magnitude than that available in the simple flow or shear mode [12]. Moreover, the yield stress of these fluids could be enhanced further if they are employed in the so-called mixed-mode operation. Recently, the authors [13] experimentally demonstrated the advantages of a mixed squeeze and shear-flow mode for enhancing the performance of ER fluids. This increased fluid strength was also confirmed [14] in a test of an MR mixed-mode compact isolator under sinusoidal vibration inputs supplied by an electromagnetic shaker for a set of mechanical frequencies in the range 2–25 Hz. In addition, a previous study [16] investigated the performance of an MR fluid isolator designed with a

relatively large single coil, which was capable of providing only a partial energization of the fluid under mixed squeeze, shear, and flow operation.

However, further work is necessary for exploiting the mechanical and electrical properties of ER and MR fluids under the mixed-mode operation. The present study was therefore focused on an experimental investigation aimed at determining the performance of an MR-fluid-based mixed-mode device, which was tested under quasi-static inputs supplied by a high-strength tensile machine. The magnetic circuit of the device, which incorporates two separate magnetic coils allowing independent and simultaneous control of the fluid areas, was designed using the ANSYS finite element software. The device was tested under single and mixed modes. The study results highlight the advantages of using MR fluids in a mixed-mode device for short-stroke isolations.

Experimental

Experimental facility

The experimental setup (Fig. 1) used for this investigation consisted of an Instron servo-hydraulic testing machine (model 4204), which is capable of vertical motion with a maximum force of 50 kN over a speed range of 0 to 520 mm/min. A dedicated cell (Fig. 2) was designed and manufactured using low-carbon steel to test the MR fluid under the single and mixed modes. The crosshead of the tensile machine was attached rigidly to a Kistler (model 9311A) piezoelectric force link and to the upper assembly (piston) of the MR fluid cell, which had a circular area, A, of approximately 6.36×10^{-3} m^2. The lower assembly of the cell, which had a recessed cavity of diameter 94 mm and served as the reservoir of the MR fluid, was rigidly connected to a second identical force link and to the supporting frame of the Instron machine. The fluid cell is open at the top and hence, the fluid is free to rise and drop along the vertical fluid path in response to fluid volume changes in the annular gap, which are initiated by piston motions. A pair of toroidally shaped electromagnetic coils, located symmetrically about

the centerline of the cell, was designed to be energized either in isolation of each other or simultaneously to enable the excitation of the fluid under the single- or mixed-mode operation, respectively. Electrical excitation of the coil was achieved by means of a quad-mode TTi (model PL330QMT) low-voltage power supply.

The instantaneous displacement, velocity, and acceleration of the piston assembly were measured using an RDP (type GTX 2500) linear variable differential transformer (LVDT), an RDP (type 240A0500) self-induced velocity sensor, and an Endevco (type 7254-100) accelerometer, respectively. Data acquisition and processing were performed using a Measurement Group (type ESAM) analog-to-digital converter with simultaneous sampling capability, which was controlled by a Pascal program running on an IBM-compatible personal computer. To perform meaningful comparisons between the results of various tests, the temperature of the MR fluid was maintained at a constant level by circulating water with a controlled temperature through a closed cavity in the lower assembly of the cell by using a Grant Instruments (model LTD6) temperature control unit.

Calibration of sensors

The two force links were calibrated statically by sequential loading using small weights, whereas the LVDT was calibrated using a micrometer calibration unit that was specifically designed for the accurate calibration of the LVDT. The accelerometer, precalibrated by the manufacturer, was found to function as specified to within $\pm 0.6\%$ when its maximum transverse sensitivity was checked using a digital sine controller. As an additional verification step, the displacement signal from the LVDT was differentiated twice using central differences and the resulting signal was found to agree well with that from the accelerometer. Finally, the data acquisition system was checked against a DC signal supplied by a millivolt calibration unit (Time Electronics, model 404S) and was found to be accurate to within $\pm$ 0.5%.

MR fluid

The MR fluid used in these experiments was a homemade suspension of carbonyl iron powder in hydrocarbon oil. The iron powder was supplied by Finetools SA with an average diameter of approximately 4 μm and a density of approximately 4.3 g/cm^3. The kinematic viscosity of the carrier oil at 20°C was 20×10^{-6} m^2/s. The weight fraction of the solid phase was approximately 80% with a magnetisation saturation in excess of 1300 kA/m. Lithium grease was added to the mixture in order to slow the settling effect of the iron particles.

Results and discussion

A systematic testing program was implemented for assessing the performance of the MR fluid under the single and mixed modes of operation by using a dedicated cell that acts as a short-stroke isolator subjected to compressive, tensile, and oscillatory motion inputs. Simultaneous measurements of the input force, F_i, delivered to the cell by the Instron tensile machine and the force transmitted, F_t, across the MR fluid, in addition to the displacement Δh, velocity V, and acceleration, a, of the cell piston, were recorded throughout the testing sequence. These measurements were recorded at a sampling frequency of 5 kHz for an input speed of approximately 1 mm/s of the tensile machine. The mean separation between the parallel plane surfaces of the piston and cylinder, h_o, was set to 2 mm (squeeze analysis). The same separation was also permitted through the annular gap between the piston and the cylinder (shear-flow analysis). Under a compressive input, the stationary piston was set to move vertically by 0.5 mm toward the plane surface of the cylinder, resulting in the displacement of the MR fluid from the circular fluid gap and its flow upward past the annular gap of the cell. In contrast, under a tensile input, the stationary piston was permitted to move upward (vertically) by 0.5 mm, which caused the fluid to flow downward through the annular gap and inward within the circular gap of the cell. For the oscillatory tests, the piston was set to oscillate by ±0.5 mm about the mean separation gap. The above tests were conducted under a

condition of constant input displacement of the tensile machine regardless of the magnetic field across the MR fluid, which was varied according to the coil excitation current ranging from 0 to 1.4 A. Although the tests were conducted for a range of MR fluid temperatures, the results presented in this paper are for the case in which the MR fluid temperature was maintained at 20°C.

Electromagnetic finite element analyses (FEA) were performed to accomplish the optimum design of the magnetic circuit that is required for energizing the MR fluid in both the squeeze and the shear-flow gaps. The electromagnetic simulations were executed using ANSYS high-accuracy electromagnetic element type "Plane 53", which is defined by 8 nodes and has up to 4 degrees of freedom per node. The element edge length was altered to increase or decrease the density of the resultant numerical mesh as judged appropriate. In addition, the mesh density was altered to increase the number of elements in certain areas including the fluid gap. The material properties were defined by assigning each material a constant relative permeability. For air and the coil area, this value was set to 1 whilst a permeability value of 1000 was set for the cell flux carrier material. The MR fluid magnetic permeability was set to 5. The last step before the model solution was executed involved the definition of the loads to which the model was subjected. This required the coil current density to be estimated which was affected by several parameters including the number of coil turns, the current supplied to the coil and the coil cross-sectional area. A self-fluxing polyurethane coated solid copper wire with a diameter of 0.71 mm was selected for the current coil design.

Figs. 3 a and b show the variation of the magnetic flux density along the median paths (shown in Fig. 2) inside the MR fluid squeeze and shear-flow gaps, respectively. In these figures, it is seen that the magnetic flux density inside the MR fluid increases with an increase in the current supplied to the coils from 0.2 A to 1.2 A. The physical boundaries of the two coils are superimposed into these figures and are represented by the projected vertical solid lines. It can be seen that the magnitude of the magnetic flux density drops along limited gap lengths in

fluid areas opposite the electromagnetic coils. This behavior is attributed to the fact that at these locations, the magnetic flux lines do not cross the fluid gaps between the piston and the cylinder, which instead results in the creation of short circuits around the coils. This effect is also clearly seen in the contour plots of the flux-line density (Figs. 4 a and b) for the squeeze and shear-flow gaps, respectively, for an input current of 0.4 A. The double-coil design proposed in the present study allows the evaluation of the device performance when it is utilized under either a single-mode operation (squeeze or shear-flow) or a mixed-mode operation (squeeze and shear-flow). Similar dual coil arrangement was utilised in a squeeze-flow mixed mode MR mount [15]. In contrast, the MR-fluid-based mixed-mode device reported by Brigley et al. [16] included a magnetic circuit with a single-coil arrangement that appeared to be capable of providing a partial excitation of the fluid in the squeeze and shear regions. The disadvantage of using a single coil arrangement was also reported by Hong et al [17] and Minh [18] in their shear-flow and squeeze-flow mixed mode devices, respectively.

Fig. 5 shows the stress Fig. 5 shows the stress ($\sigma = F_t / A$) variation of the MR structure under a compressive loading variation of the MR fluid under the squeeze mode, with the strain with the strain ($\varepsilon = \Delta h / h_o$) for coil excitation currents between 0 and 2.0 for coil excitation currents ranging between 0 and 0.8 A. In general, it can be seen that the strength of the MR viscoelastic structure seems to increase with the coil excitation current. Under compressive loading, the MR fluid initially shows an elastic deformation, which is represented by the linear portion of the stress-strain curve, and subsequently shows a plastic deformation, wherein the stress is seen to increase with the strain and attain a maximum value to mark the ultimate strength of the material before starting to decrease. This behavior could be explained by the fact that the particulate chains of the MR fluid become thicker at the early stages of the compression stroke, providing higher resistance to deformation up to the ultimate strength of the material, at which point they start to break and subsequently collapse under higher strains, causing decay of the stress. The shape of the stress-strain relationship of field-controllable

fluids under compressive stress could be affected by several factors, including its strong dependence on the initial gap size [19]. The performance of the MR fluid under the squeeze operation and tensile inputs is also shown in Fig. 5, which also displays both the elastic and the plastic regions of deformation. However, the MR fluid seems to provide higher strengths when utilized under compression, which is particularly clear within the plastic deformation region. This fluid performance is in agreement with that predicted theoretically and experimentally for ER fluids [20-22]. Similar results were found (Figs. 6 and 7) when the MR fluid was assessed under shear-flow and mixed-mode operations, respectively, although the former operation showed less dependence on the strain direction.

Fig. 8 shows the compression characteristics of the MR fluid under squeeze, shear-flow, and mixed-mode operations for excitation currents between 0.0 A and 0.8 A. It is clear that for each coil excitation level, the highest compressive stress was produced when the same current was simultaneously supplied to both coils, permitting the mixed-mode operation. However, under the shear-flow and squeeze operations, the MR fluid seemed to generate close compressive strengths. Fig. 9 shows the influence of the coil excitation current on the ultimate compressive strength of the MR fluid under the single and mixed modes. As can be seen from the figure, the ultimate compressive strength of the fluid appeared to increase almost linearly with the current and was found to reach a magnitude of about 30 kPa when a current of 1.4 A was supplied to both coils (mixed mode). However, under a single (shear-flow or squeeze) mode operation, this ultimate compressive strength reduced to about 18 kPa at the same coil excitation level (1.4 A). The enhanced fluid performance under the mixed-mode operation is consistent with results of previous investigations in which mixed-mode smart fluid cells were tested using an electromagnetic shaker system [13, 14]. As a result, using the tensile machine system in this investigation to drive the fluid cell has allowed fluid characteristics quantification at higher input force levels which was not the case in the previously reported

work [14] when the MR fluid cell was able to arrest the motion of the shaker at lower magnetic field excitations.

The tensile characteristics of the MR fluid under the three modes of operation are shown in Fig. 10. Again, the best tensile characteristics of the fluid were achieved under the mixed mode, whereas the shear-flow mode produced larger tensile strengths than the squeeze mode. This fluid performance is confirmed in Fig. 11, which shows the ultimate tensile strengths of about 33 kPa, 23 kPa, and 10 kPa for the mixed, shear-flow, and squeeze modes, respectively, under a coil excitation current of 1.4 A.

The better shear-flow performance of the fluid than its squeeze-mode performance is in agreement with previously reported results by the authors [14]. This improved performance can be explained by the fact that although the shear-flow and squeeze areas were designed to be the same, the average magnetic flux density along the shear-flow path was about 6% larger than that over the squeeze path for the same current level. In addition, the present magnetic circuit design might promote the accumulation of fluid particles on the piston wall opposite the shear coil, which might result in an added fluid effect similar to the magnetic-gradient pinch effect that was recently reported by Goncalves and Carlson [23] and hence increase the fluid strength along the shear-flow path.

Next, the oscillatory (dynamic) characteristics of the fluid cell under single and mixed-mode operations were investigated for the same coil excitation current range (0–1.4 A) when the piston displacement was controlled to ±0.5 mm. Fig. 12 shows the variation of the transmitted force with time over one vibration cycle under a coil excitation current of 1.2 A. Fluid characteristics for the zero current case are also shown in this figure. When the current was increased from 0 to 1.2 A, the transmitted force was observed to increase, since the Instron machine attempts to supply higher forces to maintain the same level of displacement. It can be seen that a 370 N peak-to-peak force was transmitted by the fluid under the mixed-mode

operation, compared to 260 N and 210 N peak-to-peak forces transmitted under the shear-flow-mode and squeeze-mode operations, respectively. Fig. 13 shows a plot of the transmitted force versus displacement hysteresis loops for an input current of 1.2 A. The whirl loops in this figure illustrate the change in the level of the transmitted force due to the development of higher yield stresses with increasing magnetic field intensities, which are higher when the fluid is utilized under the mixed-mode operation. The area of these loops indicates the amount of damping, which is represented by the energy dissipated by the MR fluid over one cycle of vibration [10]. The variation of the transmitted force with velocity is shown in Fig. 14 for the same excitation current level (1.2 A). Both the force-displacement and the force-velocity figures show a clear difference between the compression and tension phases of each cycle when the fluid performance during the compression phase, which is represented by the right half of these loops, is enhanced compared to that during the tension phase (left half of the loops). This fluid performance is in agreement with that predicted theoretically and experimentally for ER fluids [25,26] and corresponds to the behaviour of Bingham-plastics that combine the yield properties of solids with the Newtonian flow properties of fluids. In addition, the force versus velocity hysteresis cycles (Fig. 14) seem to attain maximum values which, when projected back to the force axis, may result in the yield force values [24]. These yield forces are also seen to increase with increasing applied currents (Fig. 15) when a force of approximately 30 N obtained at 0 A is increased to 122 N, 160 N, and 240 N under 1.4 A excitation for the squeeze, shear-flow, and mixed modes, respectively. Again, this fluid performance enhancement under mixed mode operation is in agreement with those reported by Sarkar and Hirani [27], Spaggiari and Dragoni [28] and Becnel et al [29] although the shearing of the fluid in their mixed squeeze-shear cells was achieved through piston rotations rather than through a direct axial motion which is realized in this investigation.

Conclusions

The MR fluid cell presented in this paper was designed to permit the assessment of the fluid under either a single (shear-flow or squeeze) mode operation or a mixed-mode operation. The mixed squeeze and shear-flow mode was found to enable the transmission of significantly larger forces through the MR fluid. This was evident under compressive and tensile motion inputs. The higher load transmission under the shear-flow mode than that under the squeeze mode is due mainly to the fact that the present magnetic circuit design produces a higher magnetic field density along the shear path than along the squeeze path, in addition to the possible accumulation of fluid particles along the shear path, thereby resulting in an added gradient pinch mode effect and hence better shear-flow performance.

The MR cell was also assessed under oscillatory (dynamic) motions, and again, the mixed-mode operation was found to result in better fluid performance than either the single shear-flow-mode operation or the single squeeze-mode operation.

The proposed MR fluid cell with its enhanced mixed-mode operation could be employed in large-scale short-stroke damping applications such as engine mounting and structural damping.

Acknowledgements

This research received no specific grant from any funding agency in the public, commercial, or not-for-profit sectors.

References

[1] Rabinow J. The magnetic fluid clutch. AIEE Transaction 1949;67:1308-1315.

[2] Winslow WM. Induced fibrillation of suspensions. J Applied Physics 1949;20:1137-1140.

[3] Hartsock DL, Novak RF, Chaundy GJ. Electrorheological fluid requirements for automotive devices. J Rheology 1991;35:1305-1326.

[4] Delphi Energy & Chassis Systems, 2002, Pub. DE-00-E-019.

[5] Johnson L. Electrorheological dampers for industrial and mobile applications – an overview of design variations, product realisation and performance. Actuator08 2008; Conference Proc., Bremen, Germany:499-502.

[6] El Wahed AK, Sproston JL, Schleyer GK. Electrorheological and magnetorheological fluids in blast resistant design applications. Materials and Design 2002;23:391-404.

[7] Liu Y, Jiang W, Jing ZS, Zhang RP, Liu ZM. Semi-active control of vehicle suspensions with MRF damper based on robust control theory. Key Engineering Materials 2011;474-476:1423-1428.

[8] Choi YT, Bitman L, Wereley NM. Nondimensional analysis of electrorheological dampers using an Eyring constitutive relationship. Collection of Technical Papers-AIAA/ASME/ASCE/AHS/ASC Structures, Structural Dynamics and Materials Conference 2004;5:4045-4058.

[9] Jang KI, Min BK, Seok J. A behavior model of a magnetorheological fluid in direct shear mode. J Magnetism and Magnetic Materials 2011;323:1324-29.

[10] El Wahed AK. The influence of solid-phase concentration on the performance of electrorheological fluids in dynamic squeeze flow. Materials and Design 2011;32:1420-26.

[11] Li R, Chen WM, Liao CR. Hierarchical fuzzy control for engine isolation via magnetorheological fluid mounts. Proceedings of the Institution of Mechanical Engineers, Part D: Journal of Automobile Engineering 2010;224:175-187.

[12] Monkman G. The electrorheological effect under compressive stress. J Phy. D: Appl. Phy. 1995;28:588-93.

[13] El Wahed AK. Performance evaluation of electrorheological fluids under mixed shear and squeeze mode. ACTUATOR08, Proc. of the 11th Int. Conf. on New Actuators, Bremen, Germany, June 9-11 2008:838-841.

[14] El Wahed AK, McEwan CM. Design and performance evaluation of magnetorheological fluids under single and mixed modes. J Intel. Material Systems and Structures 2011;22:631-43.

[15] Goldasz J, Sapinski B. Modelling of magnetorheological mounts in various operation modes. acta mechanica et automatic 2011;5:29-39.

[16] Brigley M, Choi YT, Wereley NM. Experimental and theoretical development of multiple fluid mode magnetorheological isolators. J Guidance, Control, and Dynamics 2008;31:449-459.

[17] Hong SR, Choi SB, Choi YT, Wereley NM. Non-dimensional analysis and design of a magnetorheological damper. Journal of Sound and Vibration 2005;288:847–863.

[18] Minh NT. A novel semi-active magnetorheological mount for vibration isolation, PhD Dissertation.

[19] Tian Y, Wen S, Meng Y. Compressions of electrorheological fluids under different initial gap distances. Phys. Rev. 2003;67:051501.

[20] El Wahed AK, Sproston JL, Stanway R, Williams EW. An improved model of ER fluids in squeeze-flow through model updating of the estimated yield stress. Journal of Sound and Vibration 2003;268:581-599.

[21] Gong H, Lim MK. Experimental investigations on tension and compression properties of an electro-rheological material. J Intelligent Material Systems and Structures 1996;7:89-96.

[22] Lukharinen A, Kaski K. Computational studies of compressed and sheared electrorheological fluid. J Physics D: Applied Physics 1996;29:2729-2732.

[23] Goncalves FD, Carlson JD. An Alternative Operation Mode for MR Fluids: Magnetic Gradient Pinch. Journal of Physics: Conference Series 2009;149:012050.

[24] Pang L, Kamath GM, Wereley NM. Analysis and testing of a linear stroke magnetorheological damper. AIAA/ASME Adaptive Structure Forum, Long Beach CA, Paper no AIAA 98-2040, 1997.

[25] El Wahed AK, Stanway R, Sproston JL. The influence of mechanical input amplitude on the dynamic response of an electrorheological fluid in squeeze flow. International Journal of Vehicle Design 2003;33:153–170.

[26] Choi SB and Kim KS. Tensile and compressive behaviours of smart electrorheological materials. Key Eng. Mater 2005;297–300:646–652.

[27] Sarkar C, Hirani H. Theoretical and experimental studies on a magnetorheological brake operating under compression plus shear mode. Smart Materials and Structures 2013;22:115032.

[28] Spaggiari A, Dragoni E Combined squeeze-shear properties of magnetorheological fluids: Effect of pressure. Journal of Intelligent Material Systems and Structures 2014;25:1041–1053.

[29] Becnel AC, Sherman SG, Hu W, Wereley NM. Squeeze strengthening of magnetorheological fluids using mixed mode operation. Journal of Applied Physics 2015;117:17C708.

Figure Captions

Fig. 1. Experimental setup

Fig. 2. MR fluid cell

Fig. 3a. Magnetic field distribution through median path inside MR fluid squeeze mean gap

Fig. 3b. Magnetic field distribution through median path inside MR fluid shear-flow gap

Fig. 4a. Contour plot of flux-line density of MR fluid in squeeze section

Fig. 4b. Contour plot of flux-line density of MR fluid in shear-flow section

Fig. 5. Comparison between compressive and tensile stresses of MR fluid under squeeze mode

Fig. 6. Comparison between compressive and tensile stresses of MR fluid under shear-flow mode

Fig. 7 Comparison between compressive and tensile stresses of MR fluid under mixed mode

Fig. 8. Comparison among squeeze, shear-flow, and mixed modes under compressive input

Fig. 9. Ultimate strength of MR fluid for single and mixed modes under compressive input.

Fig. 10. Comparison among squeeze, shear-flow, and mixed modes under tensile input

Fig. 11. Ultimate strength of MR fluid for single and mixed modes under tensile input

Fig. 12. Variation of transmitted force with time for single and mixed modes under oscillatory motion

Fig. 13. Variation of transmitted force with displacement for single and mixed modes under oscillatory motion

Fig. 14. Variation of transmitted force with velocity for single and mixed modes under oscillatory motion

Fig. 15. Variation of yield force with current for MR fluid under single and mixed modes

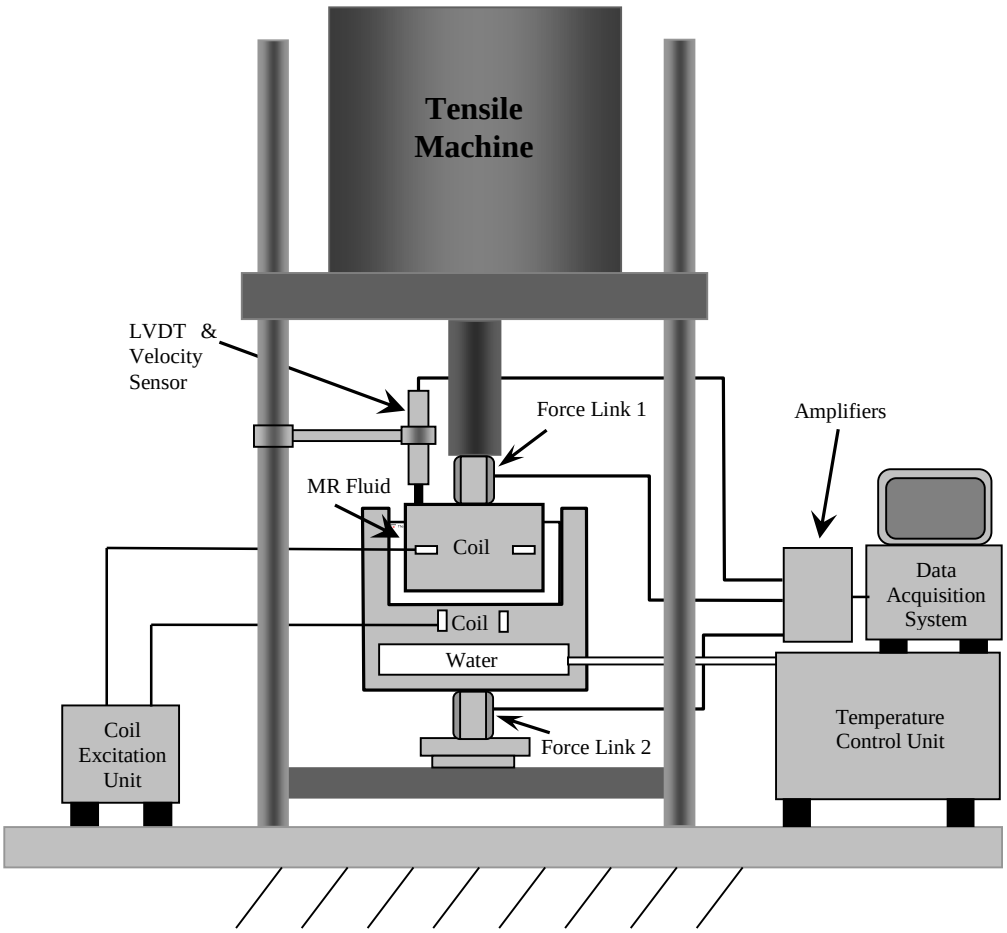

Fig. 1. Experimental setup.

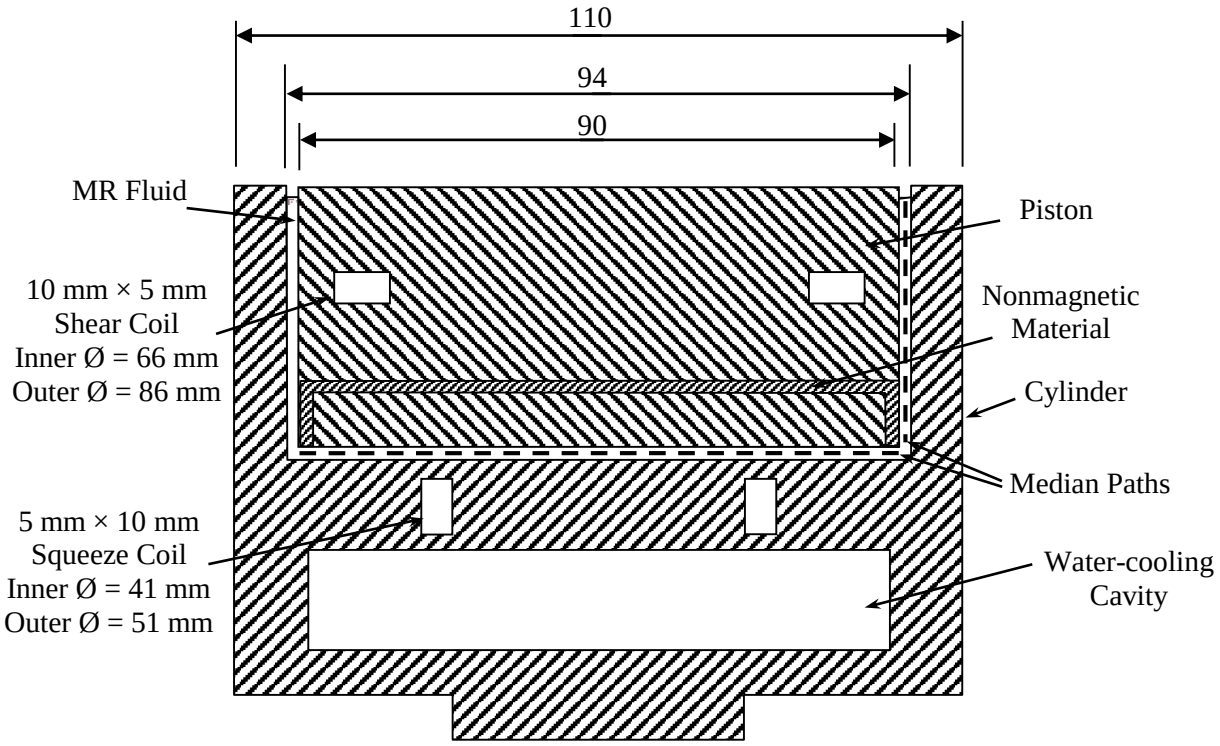

Fig. 2. MR fluid cell.

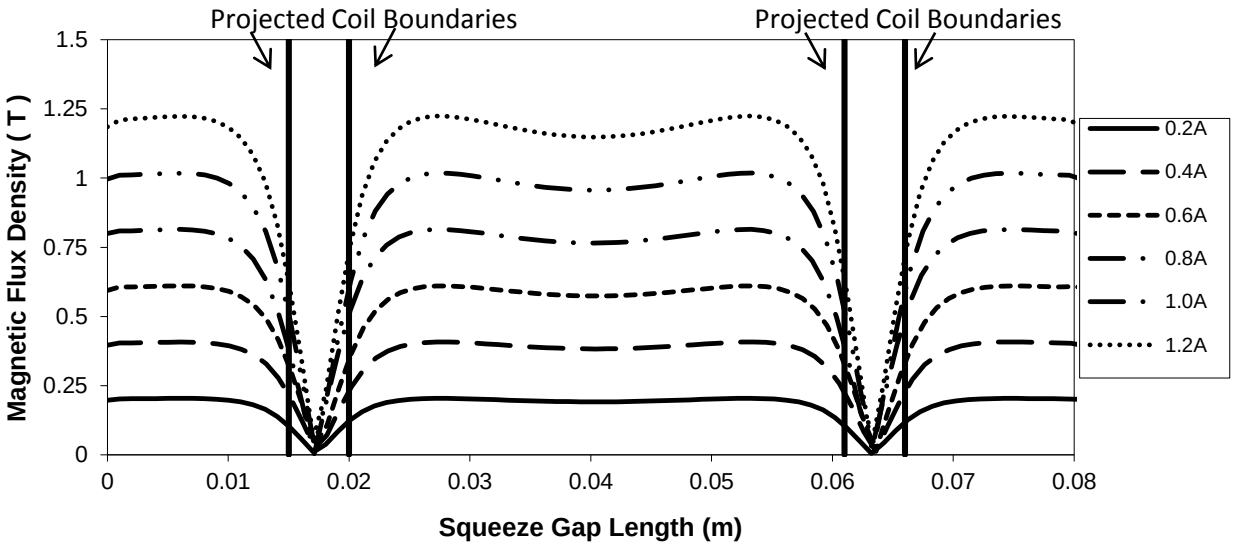

Fig. 3a. Magnetic field distribution through median path inside MR fluid squeeze mean gap.

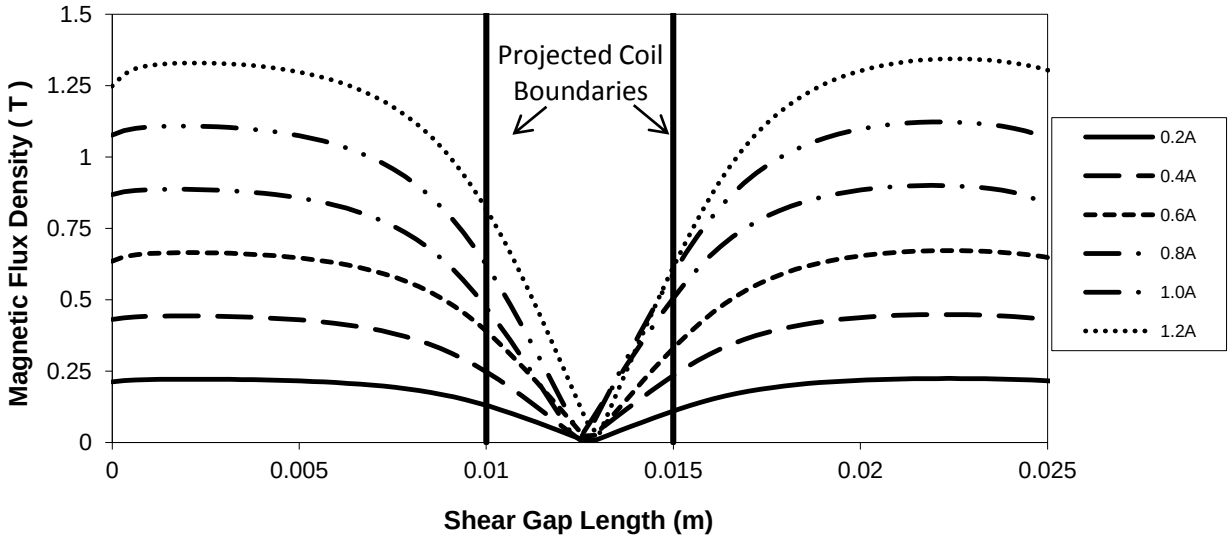

Fig. 3b. Magnetic field distribution through median path inside MR fluid shear-flow gap.

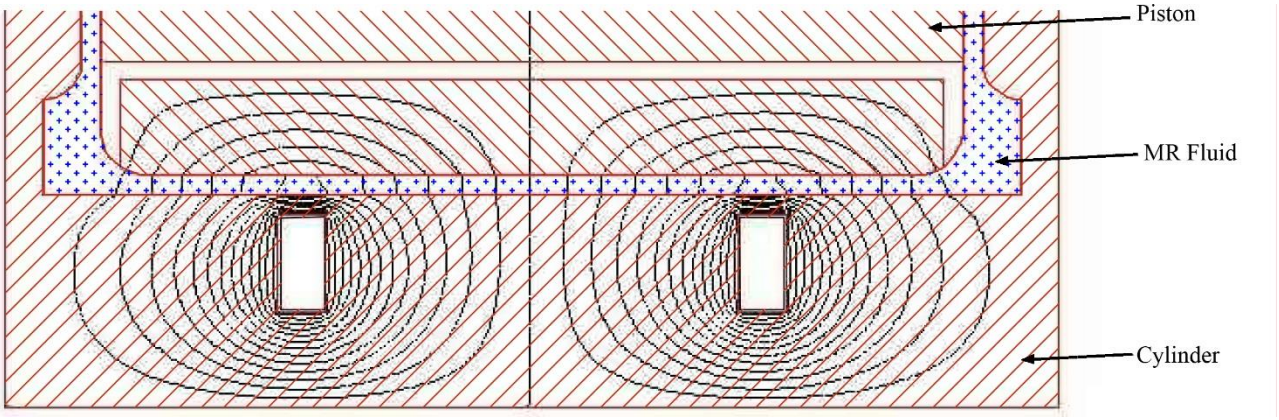

Fig. 4a. Contour plot of flux-line density of MR fluid in squeeze section.

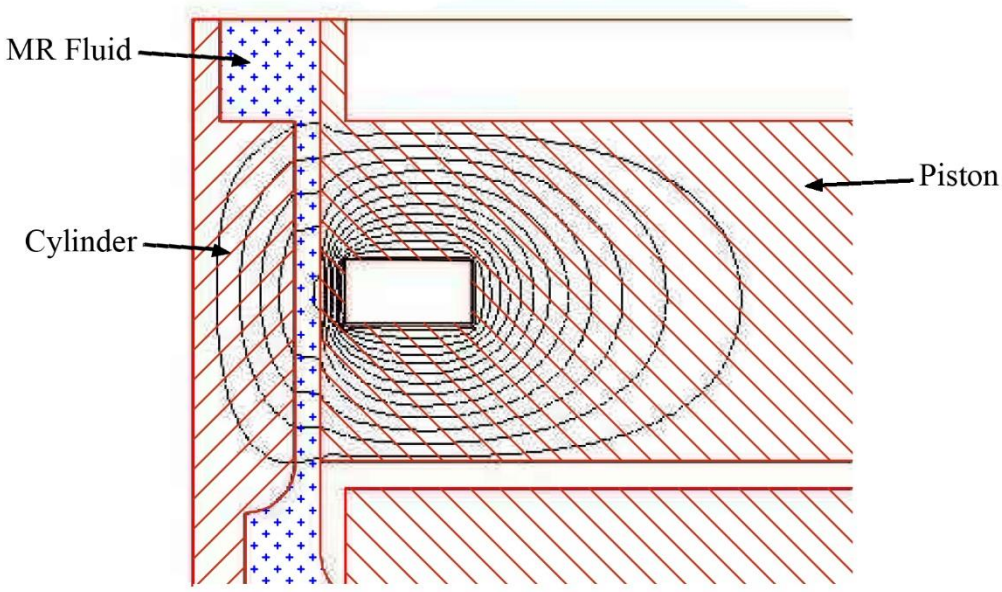

Fig. 4b. Contour plot of flux-line density of MR fluid in shear-flow section.

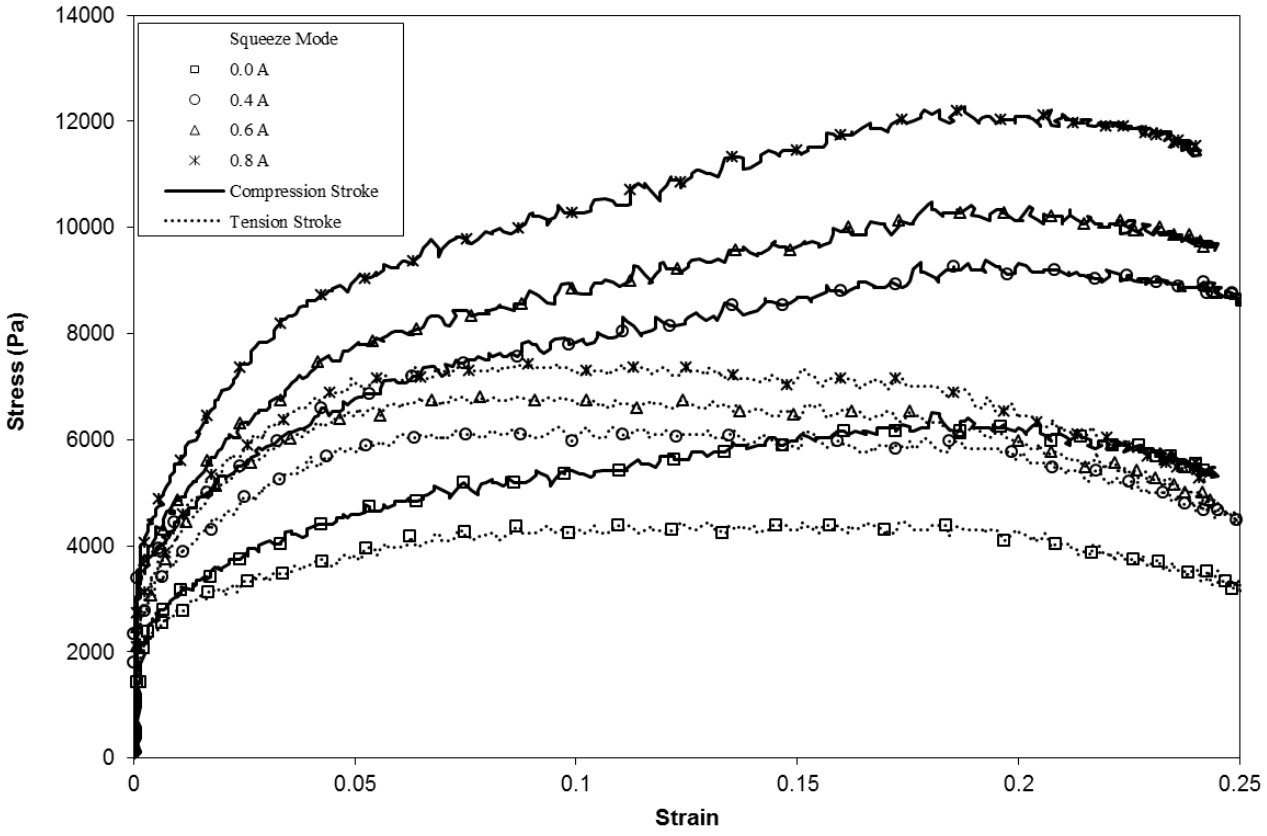

Fig. 5. Comparison between compressive and tensile stresses of MR fluid under squeeze mode.

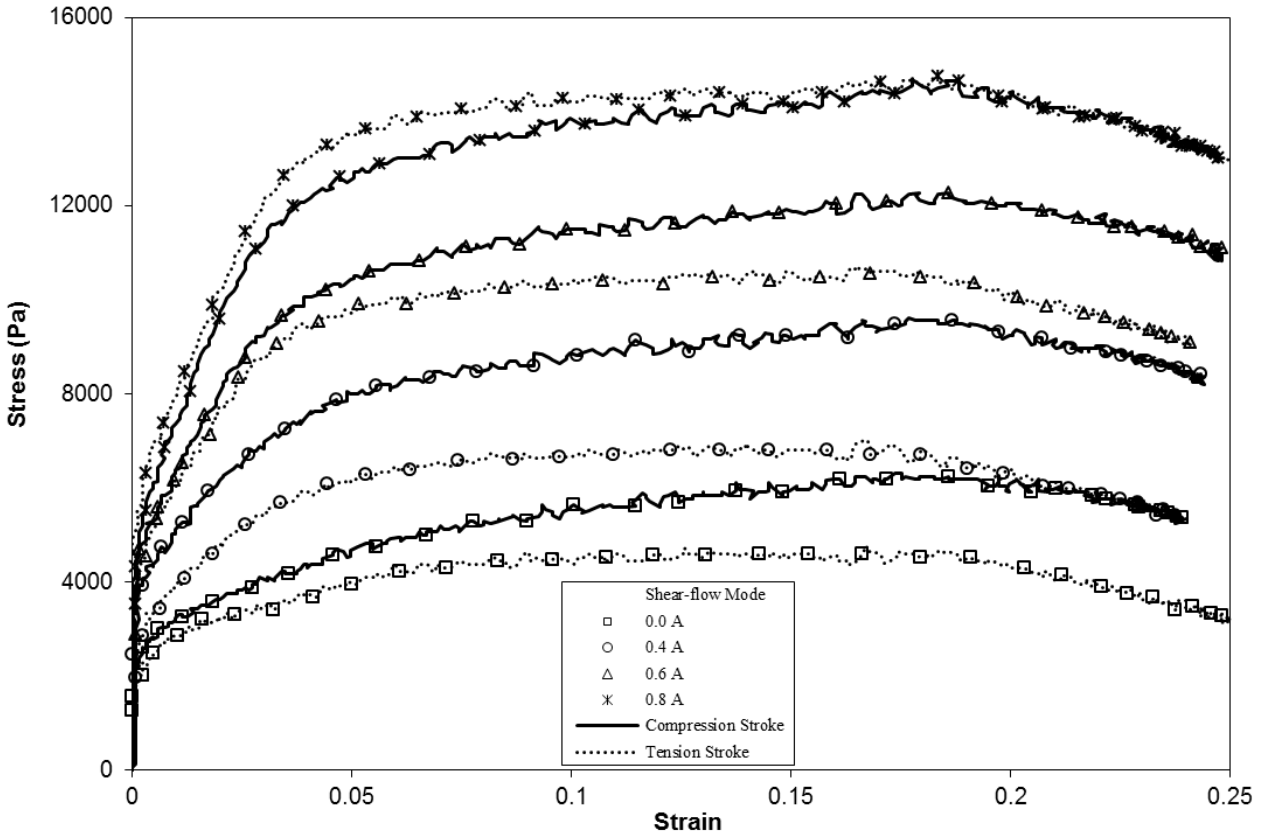

Fig. 6. Comparison between compressive and tensile stresses of MR fluid under shear-flow mode.

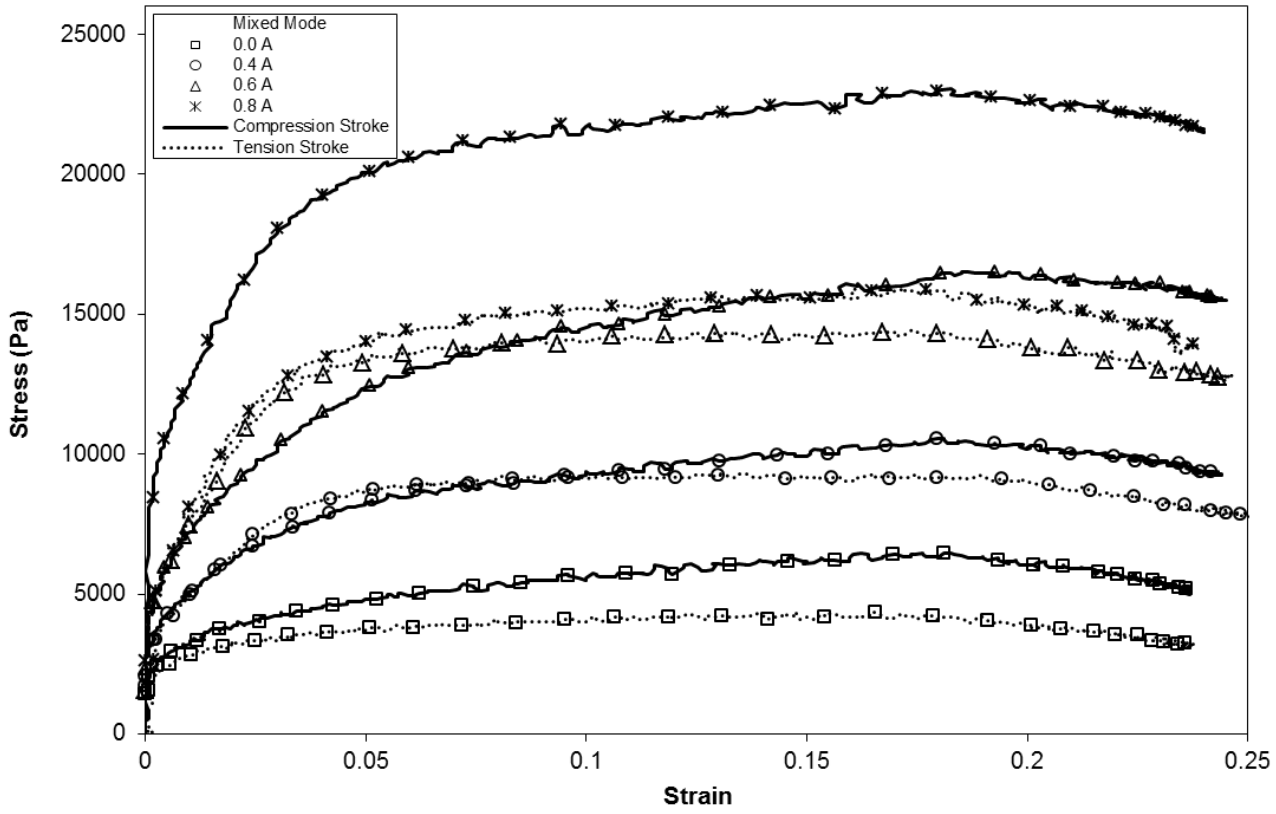

Fig. 7. Comparison between compressive and tensile stresses of MR fluid under mixed mode.

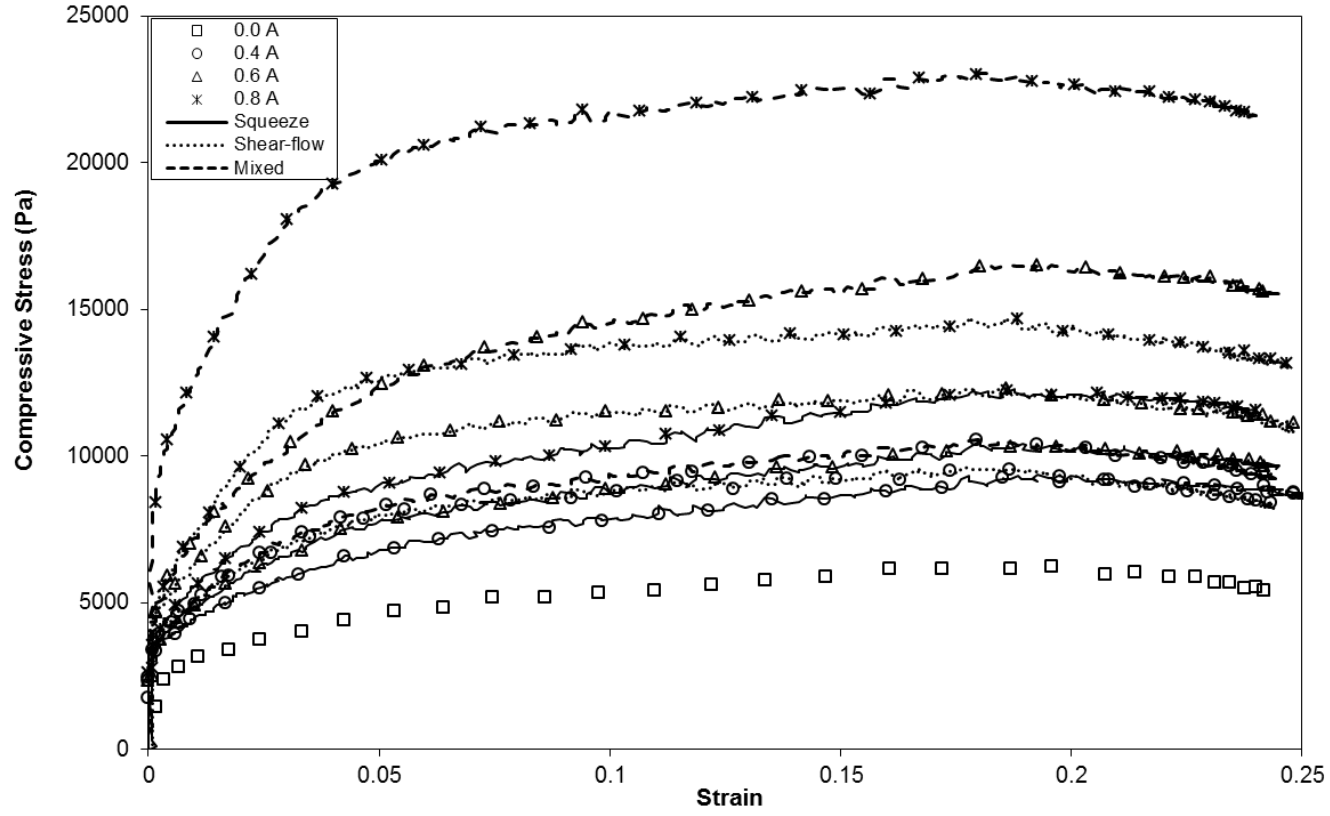

Fig. 8. Comparison among squeeze, shear-flow, and mixed modes under compressive input.

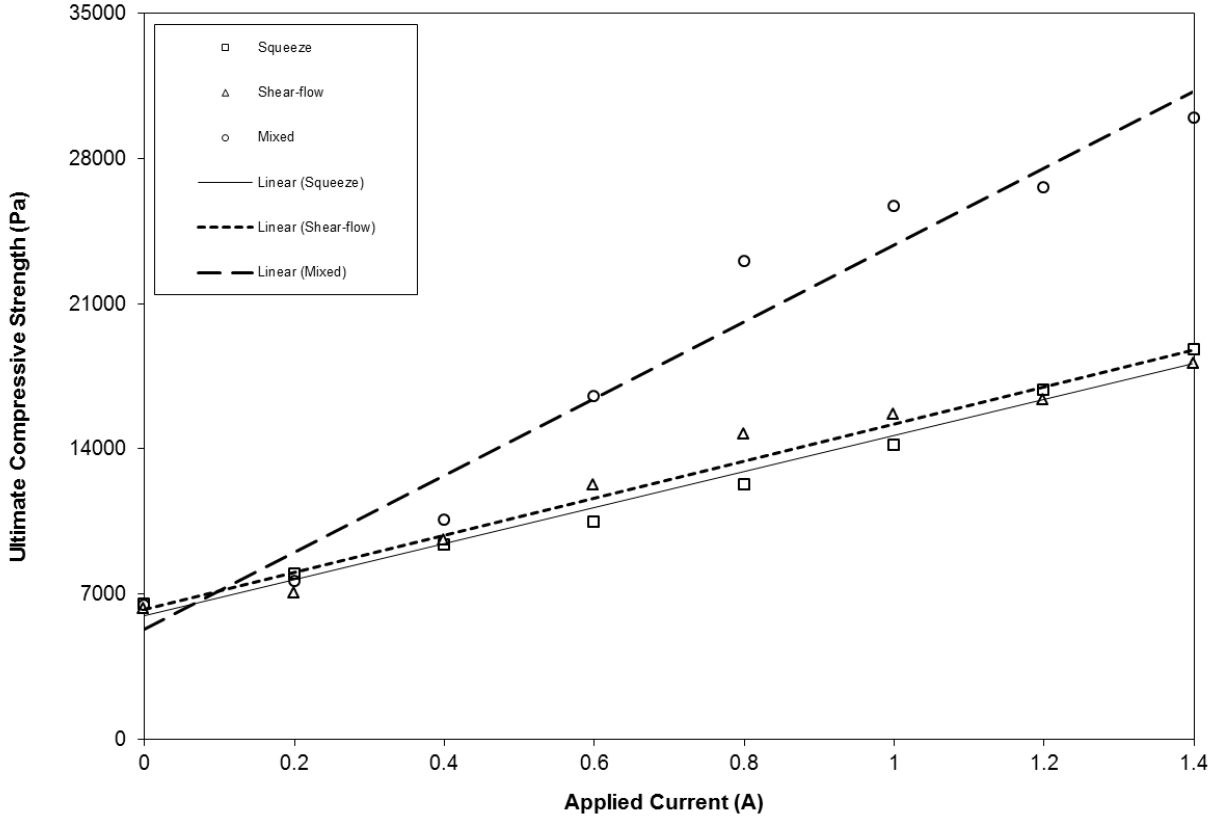

Fig. 9. Ultimate strength of MR fluid for single and mixed modes under compressive input.

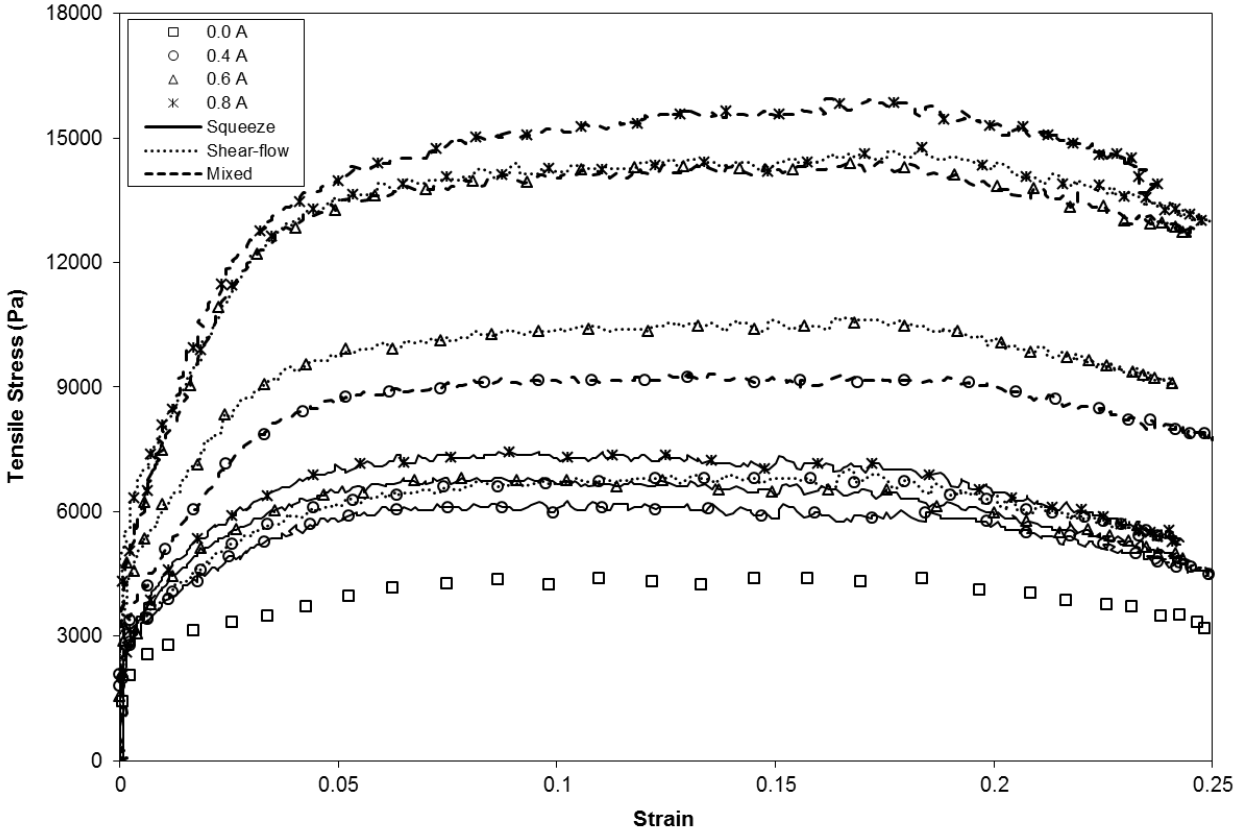

Fig. 10. Comparison among squeeze, shear-flow, and mixed modes under tensile input.

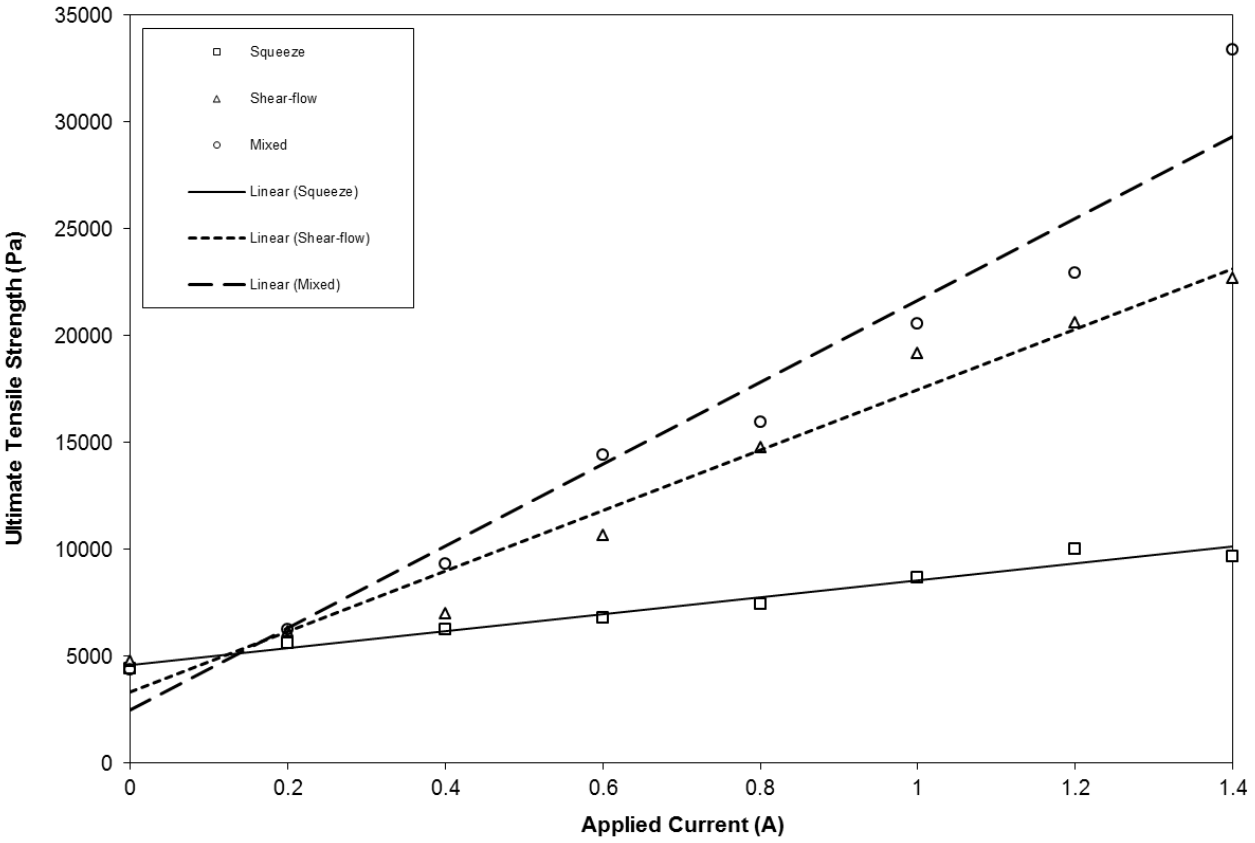

Fig. 11. Ultimate strength of MR fluid for single and mixed modes under tensile input.

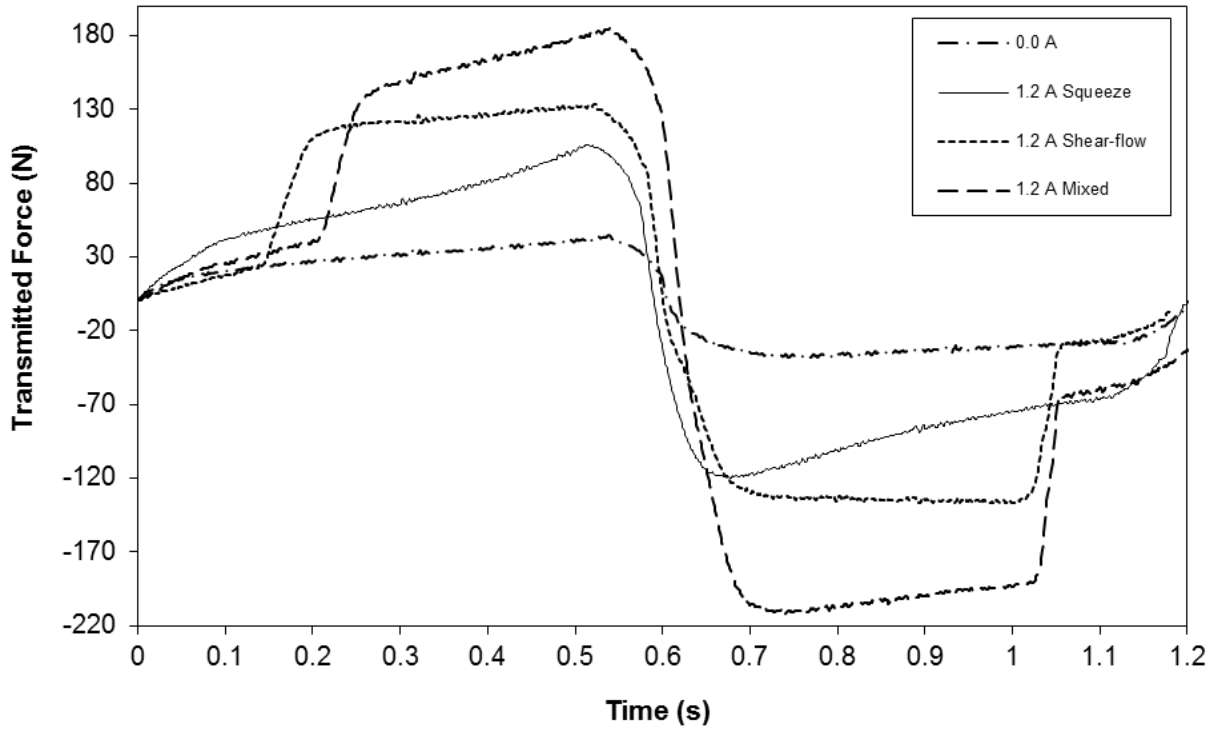

Fig. 12. Variation of transmitted force with time for single and mixed modes under oscillatory motion.

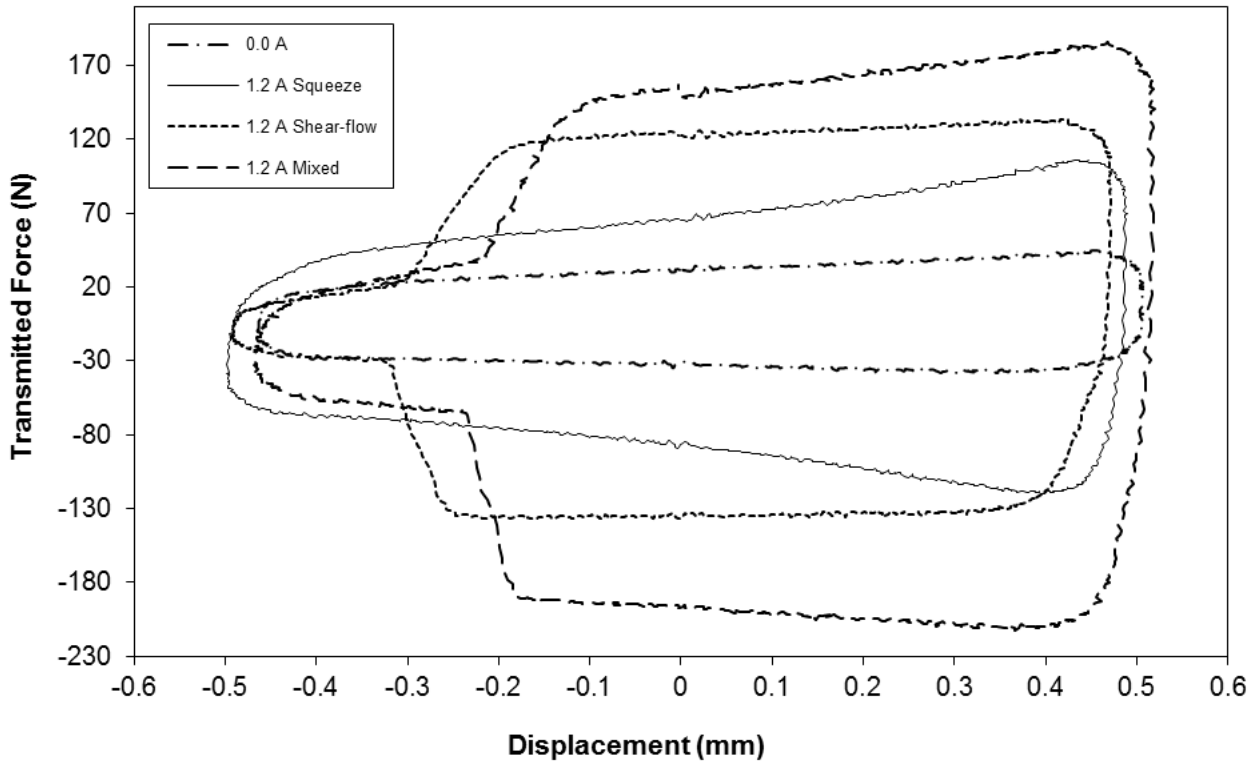

Fig. 13. Variation of transmitted force with displacement for single and mixed modes under oscillatory motion.

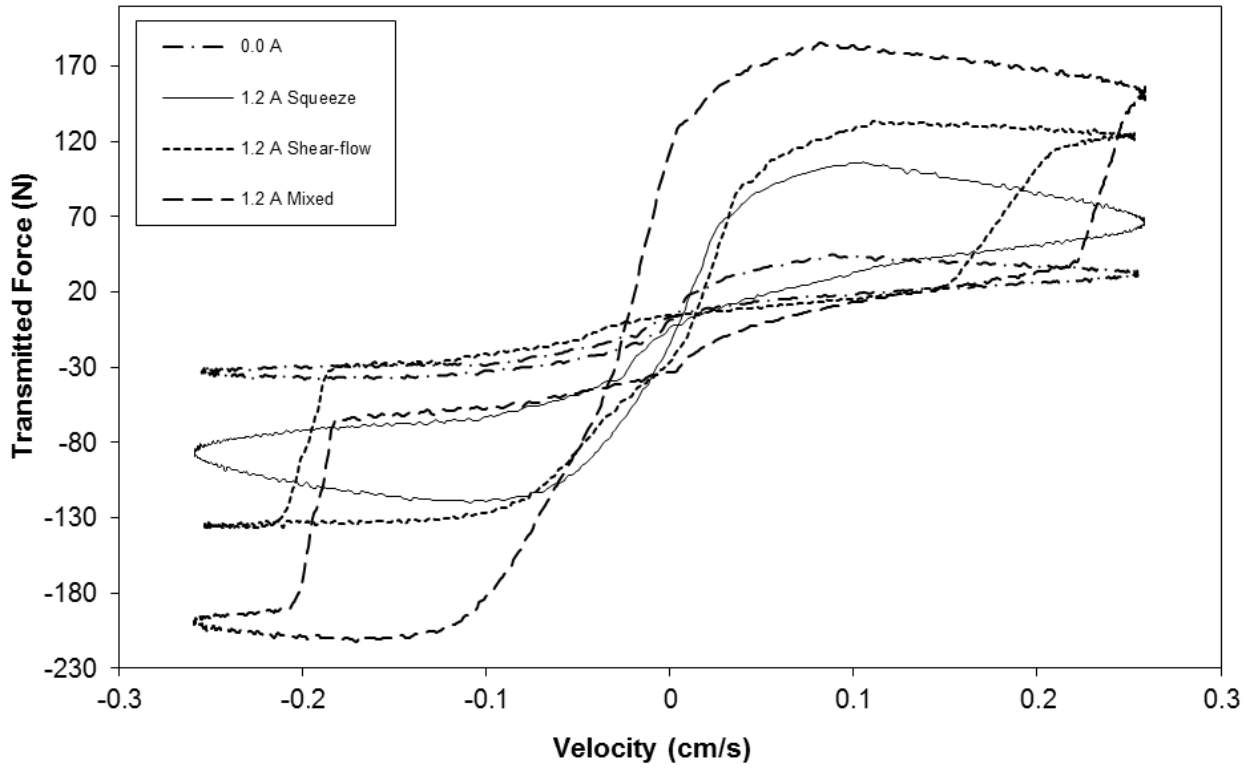

Fig. 14. Variation of transmitted force with velocity for single and mixed modes under oscillatory motion.

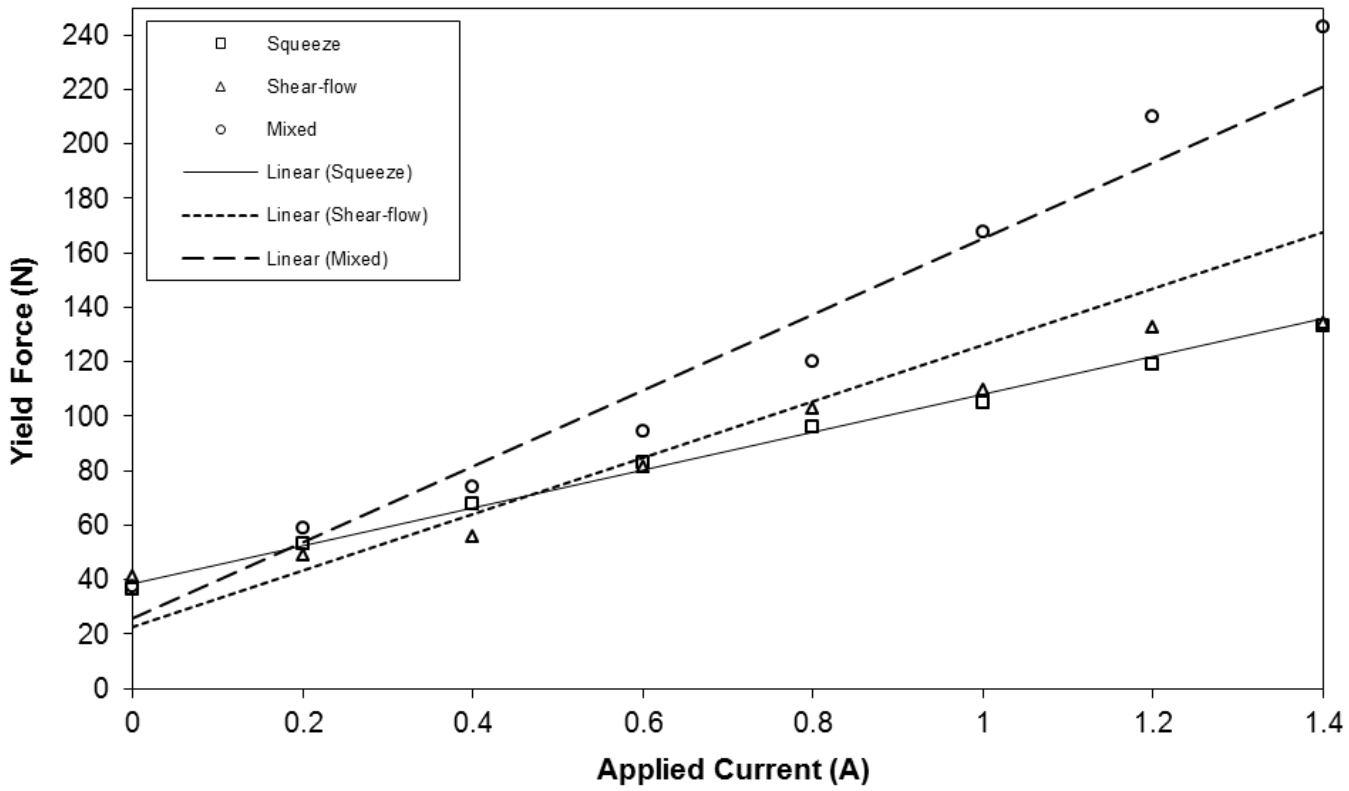

Fig. 15. Variation of yield force with current for MR fluid under single and mixed modes.